Graphitization process of SiC(0001) studied by electron energy loss spectroscopy

T. Langer, H. Pfnür, H. W. Schumacher, and C. Tegenkamp

Citation: Appl. Phys. Lett. **94**, 112106 (2009);
View online: https://doi.org/10.1063/1.3100776
View Table of Contents: http://aip.scitation.org/toc/apl/94/11
Published by the American Institute of Physics

Graphitization process of SiC(0001) studied by electron energy loss spectroscopy

T. Langer,[1,2] H. Pfnür,[1] H. W. Schumacher,[2] and C. Tegenkamp[1,a)]
[1]*Institut für Festkörperphysik, Leibniz Universität Hannover, Appelstraße 2, D-30167 Hannover, Germany*
[2]*Physikalisch–Technische Bundesanstalt, Bundesallee 100, D-38116 Braunschweig, Germany*

(Received 22 December 2008; accepted 26 February 2009; published online 16 March 2009)

Electron energy loss spectroscopy (EELS) is used to study the transition from the buffer layer to the first graphene layers during graphitization of SiC(0001). Graphene growth is controlled and correlated with spot profile analysis in low energy electron diffraction and x-ray photoelectron spectroscopy. In the EELS data both electronic transitions and plasmon losses are sensitive to the interface. The collective in-plane excitations show a characteristic blueshift upon graphitization, while single electron transitions with dipole moments along the surface normal are suppressed for the buffer layer. These dependencies can be used to control the number of epitaxially grown graphene layers. © *2009 American Institute of Physics*. [DOI: 10.1063/1.3100776]

The potential of single graphene layers has stimulated many research activities within the past years since the discovery by the Manchester group.[1] The amazing attribute that single atomic layers are stable with a truly two-dimensional (2d) electronic system[2] results in quantum transport phenomena and has been demonstrated up to now only for exfoliated graphene layers on SiO_2 substrates.[1,3]

However, the growth of graphene films under ultrahigh vacuum conditions on well-defined surfaces is a necessity in order to obtain large scale graphene templates for future applications, and several attempts have been made recently, e.g., transition metal surfaces (Ir and Ru) are used to grow single, almost defect-free graphene layers simply by thermal decomposition of hydrocarbon gases.[4,5] An alternative approach, which potentially also allows transport measurements, is the use of either Si- or C-rich insulating SiC(0001) surfaces. A carbon rich phase on top is generated by a temperature driven segregation process, which finally results in the growth of single graphene layers upon further annealing.[6–8]

In the case of SiC(0001) the structure of the graphene-SiC interface is currently extensively discussed. Apparently the Dirac point, providing those massless Dirac fermions for mesoscopic transport phenomena,[9] is seen only starting with the second graphene layer. Based on the latest first-principles calculations and scanning tunneling microscopy (STM) investigations, a model is suggested,[10,11] which explains convincingly the discrepancy found in low energy electron diffraction (LEED) and STM measurements.[12–14] Although this so-called buffer layer exhibits locally graphene lattice symmetry, there are strong remaining C–Si σ bonds. The still intact π-bonds within the buffer layer are responsible for the quasi-(6×6) corrugation seen in STM and LEED.[8,12] These Si–C bonds might cause a gap opening at the *K*-point, in agreement with angle resolved photoemission spectroscopy (ARPES).[15] They explain also the spacial variation in the surface potential, seen by STM and atomic force microscopy.[11,16] In order to grow single layer graphene on SiC that is suitable for transport experiments, the transition from the buffer layer to the first graphene layer must be monitored accurately, which turned out to be difficult using the methods discussed in the literature so far.

In this letter we report on electron energy loss spectroscopy (EELS) measurements in reflection, which are extremely surface sensitive, in contrast to absorption experiments done with light or EELS in transmission. The optical properties of graphite and its allotropes, e.g., nanotubes and C_{60} molecules, have been investigated extensively.[17,18] From these investigations, a detailed understanding of their electronic loss structure has been obtained. It can be understood in terms of single electronic transitions and collective excitations, i.e., plasmons. The graphitization process of SiC was studied with EELS already by Muehlhoff *et al.*[19] two decades ago. However, the appearance of these losses in the limit of single graphene layers has not been considered yet. As will become apparent by analyzing dipole-allowed electronic transitions, the graphenelike buffer layer can be well distinguished from graphene layers thus providing a tool to control also the formation of single layer graphene on SiC.

All measurements were performed under UHV condition at 100 K substrate temperature. The pressure during the sublimation process did not exceed 8×10^{-10} mbar. In order to calibrate the number of graphene layers in our study, spot-profile analysis of LEED [SPALEED (Ref. 12)] and x-ray photoelectron spectroscopy (XPS),[7] available in the same UHV system, was used. The temperatures were measured with an IR-pyrometer (Impac, $\epsilon=0.99$). As substrate, we used Si-terminated 6*H*-SiC(0001) samples (*n*-doped, $\approx10^{18}$ cm^{-3} from SiCrystal AG), which were etched in a furnace with H_2-atmosphere in order to remove the residual roughness from polishing steps. After degassing the sample at 900 °C for 12 h, we obtained instantaneously a LEED pattern showing the Si-rich (3×3) and $(\sqrt{3}\times\sqrt{3})$ structures [cf. with Fig. 1(a)]. Annealing to 1050 °C for 15 min leads to sublimation of Si and to the formation of a C-rich $(6\sqrt{3}\times6\sqrt{3})$ in coexistence with $(\sqrt{3}\times\sqrt{3})$, the precursor state for the buffer layer [Fig. 1(b)].[12,20] Heating the sample further, results first in the growth of the above mentioned buffer layer. According to Ref. 12, an indication for the formation of this graphenelike layer, which has been used in the past to calibrate the layer thickness, is the vanishing of the

a)Electronic mail: tegenkamp@fkp.uni-hannover.de.

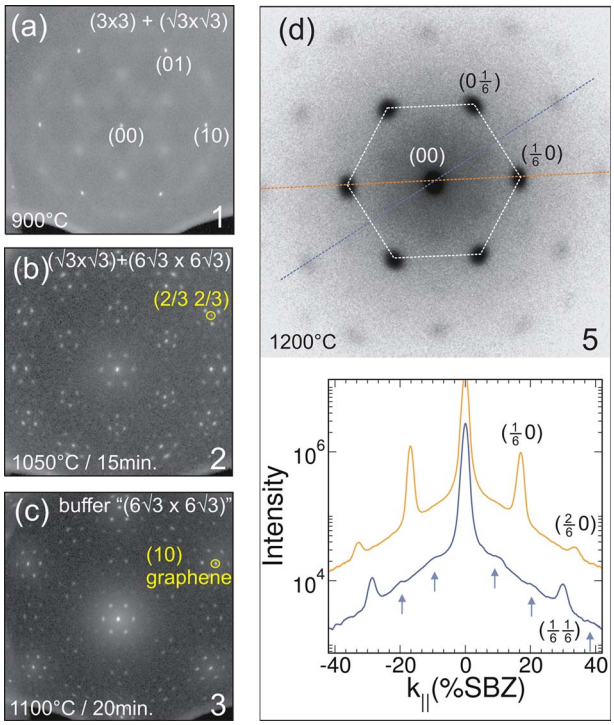

FIG. 1. (Color online) LEED pattern taken at 140 eV after different annealing steps revealing characteristic reconstructions: (a) $(\sqrt{3}\times\sqrt{3})$ after degassing, (b) $(6\sqrt{3}\times6\sqrt{3})$ in coexistence with $(\sqrt{3}\times\sqrt{3})$, and (c) buffer layer. (d) LEED pattern (contrast inverted) of the (00) spot of a 2 ML graphene film. The corresponding line scans still show the quasi-(6×6) and $(6\sqrt{3}\times6\sqrt{3})$ (arrows) symmetry of the underlying buffer layer.

$\left(\frac{2}{3}\frac{2}{3}\right)$-spots and the appearance of integer order spots of the graphene lattice [cf. with circles Fig. 1(c)]. Graphene layers were finally grown on the buffer layer at higher annealing temperatures and/or longer annealing times.

Although the (6×6) periodicity is dominant in STM at low bias voltages and in LEED, the $(6\sqrt{3}\times6\sqrt{3})$ reconstruction of the long-range commensurate buffer layer was found using high resolution SPALEED, in agreement with first-principles calculations.[10] Figure 1(d) shows the vicinity of the (00)-diffraction spot of a 2 ML graphene film. Besides the diffraction spots of the long-range ordered (6×6) reconstruction, diffraction spots of the $(6\sqrt{3}\times6\sqrt{3})$ reconstruction are clearly visible. This phase can be seen better in the line scans shown in the lower part. Although the electronic modulation induced by the intact π-system is much stronger than the structural modulation of the buffer layer, symmetry is preserved by further graphene layers on top.

In order to estimate the overall graphene coverage and calibrate the signatures from LEED, the graphitization was monitored by XPS as well (Fig. 2). Compared with the C 1*s* photopeak of the bulk terminated SiC structure, we see two characteristic peaks, S1 and S2, emerging at 1.3 and 2.3 eV higher binding energies, while the $(6\sqrt{3}\times6\sqrt{3})$ reconstruction is formed. The two surface peaks were attributed to two inequivalent sp^2 and sp^3 hybridized C atoms within the $(6\sqrt{3}\times6\sqrt{3})$ reconstruction.[7] From the attenuation shown in Fig. 2(b) of both the Si 2*p* (mean-free path, $\lambda=4.1$ nm) and the SiC fraction within the C 1*s* [cf. with dashed curve in Fig. 2(a), $\lambda=3.8$ nm] photopeak, we could consistently determine the coverage for each phase during the graphitization process (±0.3 ML).

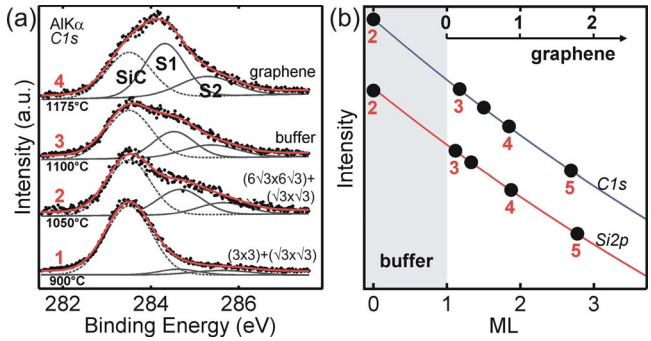

FIG. 2. (Color online) (a) Sequence of XP-spectra of the C 1*s* photopeak taken during the graphitization process. The peaks S1 and S2 can be attributed to sp^2 and sp^3 hybridized C atoms within the buffer and graphene layers. (b) From the attenuation of the SiC fraction of the C 1*s* peak and the Si 2*p* peak the corresponding thickness of the layers have been calculated, as shown in the right. Normally the buffer layer is assigned as the zeroth layer. The numbers correlate with those in Fig. 1.

In order to elucidate electronic excitations within these differently coordinated graphene layers, EELS measurements were performed. In the following we consider measurements taken at the Γ-point (30° with respect to the surface normal) for two characteristic electron energies [150 and 40 eV, Figs. 3(a) and 3(b), respectively] that reveal all important transitions. The pronounced loss peak around 6 eV can be attributed to a π-valence band plasmon, while the loss peak around 25 eV stems from a so-called $\pi+\sigma$-plasmon.[21,22] As the involved electronic states have odd parity, this loss belongs to an in-plane excitation. These modes can be only excited because the dipole fields are not completely screened by the nonmetallic substrate underneath.[23] The precipitation of additional graphene layers is seen in both plasmon losses by a blueshift as the thickness increases. The $\pi+\sigma$-plasmon located at 23 eV shifts up to 25 eV for the 2 ML graphene, close to the value seen for graphite (27 eV).[19]

Besides these plasmons, there are losses due to $\pi\rightarrow\sigma^*$ and $\sigma\rightarrow\pi^*$ single electron transitions, marked by rectangles

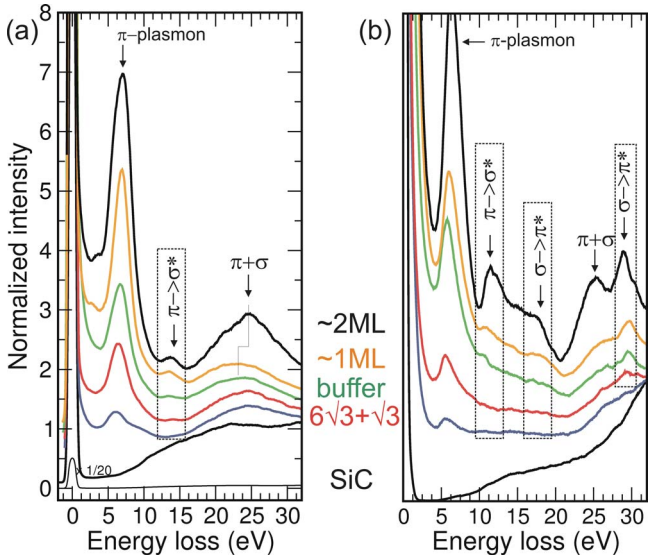

FIG. 3. (Color online) Sequence of EELS spectra taken after different steps of the graphitization process for (a) $E_p=150$ eV and (b) $E_p=40$ eV. The spectra (shifted for better visibility) are normalized with respect to the loss intensity at 25 eV. The losses marked by rectangles are due to single electron excitations.

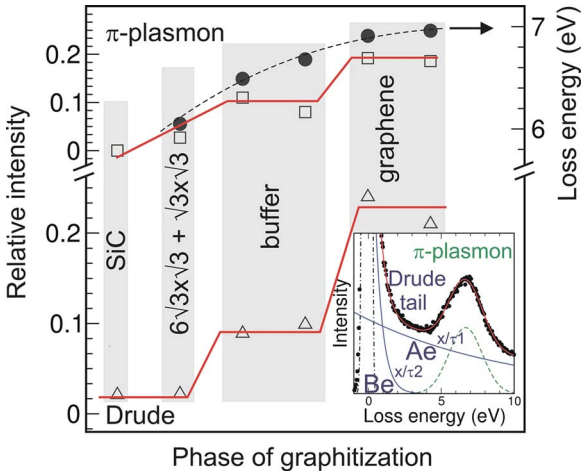

FIG. 4. (Color online) Gradual blueshift of the π-plasmon resonance (●) as a result of graphitization. The relative intensities of the plasmon (□) and the Drude tails (△) increase stepwise. In order to describe the loss intensity in between the π-loss and the specular reflex properly, the Drude tail was parameterized by two exponential functions. The relative integral intensities and peak positions were obtained by fitting the loss spectra of Fig. 3(a) like it is shown in the inset for the spectrum of a buffer layer.

in Fig. 3 and seen best at low primary electron energies. Within the dipole approximation, these excitations have dipole components only along the surface normal.[22] Interestingly, these out-of-plane single electron excitations turn out to be strongly damped or even suppressed for the buffer layer and thus can be used easily to distinguish between buffer and graphene layers.

In order to quantify the influence of the substrate and the buffer layer on graphene properties, the loss energy regime up to 10 eV has been fitted assuming Gaussian functions for the elastic peak and the π-plasmon and exponentially decaying functions accounting for the Drude tails, as shown in the inset of Fig. 4. The results for the π-plasmon and the Drude background are summarized and correlated with the different phases (deduced from LEED and XPS) in Fig. 4. The π-plasmon shifts in position gradually by about 1 to 6.9 eV as a result of graphitization. Compared to free-standing graphene sheets the residual screening by the SiC substrate and the π-system of the buffer layer prevents a shift down to the theoretical value of 4.8 eV.[18,21,22] Hence, the identification of the buffer and the graphene layer, respectively, is difficult from the inspection of the loss energy alone. The integral intensities, on the contrary, of both the π-plasmon loss and the Drude tail are much more specific. In particular, the sudden increase in the Drude background when the first graphene layer appears on the buffer layer is a characteristic of the zero-gap electronic band structure at the *K*-point of graphene,[15] while the buffer layer itself is less metallic.

In summary, we studied the graphitization process by means of EELS. The correlation with SPALEED and XPS data allows identification of the buffer layer and discrimination from the graphene layers on top. In particular, we have revealed the $(6\sqrt{3}\times 6\sqrt{3})$ symmetry of the buffer layer by SPALEED. Electronically clear differences between buffer layer and graphene were found in the single electron transitions and in the Drude tail, whereas they are more subtle for the plasmonic excitations.

[1] K. S. Novoselov, A. K. Geim, S. V. Morozov, D. Jiang, Y. Zhang, S. V. Dubonos, I. V. Grigorieva, and A. A. Firsov, Science **306**, 666 (2004).
[2] T. Ohta, A. Bostwick, Th. Seyller, K. Horn, and E. Rotenberg, Science **313**, 951 (2006).
[3] A. K. Geim and K. S. Novoselov, Nature Mater. **6**, 183 (2007).
[4] J. Coraux, A. T. N'Diaye, C. Busse, and T. Michely, Nano Lett. **8**, 565 (2008).
[5] P. W. Sutter, J. I. Flege, and E. A. Sutter, Nature Mater. **7**, 406 (2008).
[6] H. Hibino, H. Kageshima, F. Maeda, M. Nagase, Y. Kobayashi, and H. Yamaguchi, Phys. Rev. B **77**, 075413 (2008).
[7] K. V. Emtsev, Th. Seyller, F. Speck, L. Ley, P. Stojanov, J. D. Riley, and R. G. C. Leckey, Mater. Sci. Forum **556**, 525 (2007).
[8] J. Hass, W. A. de Heer, and E. H. Conrad, J. Phys.: Condens. Matter **20**, 323202 (2008).
[9] C. Berger, Z. Song, X. Li, X. Wu, N. Brown, C. Naud, D. Mayou, T. Li, J. Hass, A. N. Marchenkov, E. H. Conrad, P. N. First, and W. A. de Heer, Science **312**, 1191 (2006).
[10] S. Kim, J. Ihm, H. J. Choi, and Y.-W. Son, Phys. Rev. Lett. **100**, 176802 (2008).
[11] L. Vitali, C. Riedl, R. Ohmann, I. Brihuega, U. Starke, and K. Kern, Surf. Sci. Lett. **602**, L127 (2008).
[12] C. Riedl, U. Starke, J. Bernhardt, M. Franke, and K. Heinz, Phys. Rev. B **76**, 245406 (2007).
[13] P. Lauffer, K. V. Emtsev, R. Graupner, Th. Seyller, L. Ley, S. A. Reshanov, and H. B. Weber, Phys. Rev. B **77**, 155426 (2008).
[14] K. V. Emtsev, F. Speck, Th. Seyller, L. Ley, and J. D. Riley, Phys. Rev. B **77**, 155303 (2008).
[15] S. Y. Zhou, G.-H. Gweon, A. V. Fedorov, P. N. First, W. A. de Heer, D.-H. Lee, F. Guinea, A. H. Castro Neto, and A. Lanzara, Nature Mater. **6**, 770 (2007).
[16] T. Filleter, K. V. Emtsev, Th. Seyller, and R. Bennewitz, Appl. Phys. Lett. **93**, 133117 (2008).
[17] T. Pichler, M. Knupfer, M. S. Golden, J. Fink, A. Rinzler, and R. E. Smalley, Phys. Rev. Lett. **80**, 4729 (1998).
[18] A. G. Marinopoulos, L. Wirtz, A. Marini, V. Olevano, A. Rubio, and L. Reining, Appl. Phys. A: Mater. Sci. Process. **78**, 1157 (2004).
[19] L. Muehlhoff, W. J. Choyke, M. J. Bozack, and J. T. Yates, J. Appl. Phys. **60**, 2842 (1986).
[20] C. Riedl, A. A. Zakharov, and U. Starke, Appl. Phys. Lett. **93**, 033106 (2008).
[21] T. Eberlein, U. Bangert, R. R. Nair, R. Jones, M. Gass, A. L. Bleloch, K. S. Novoselov, A. Geim, and P. R. Briddon, Phys. Rev. B **77**, 233406 (2008).
[22] D. L. Greenaway, G. Harbeke, F. Bassani, and E. Tosatti, Phys. Rev. **178**, 1340 (1969).
[23] F. P. Netzer and J. A. D. Matthew, Solid State Commun. **29**, 209 (1979).